

Quantum Erasure and Coherence Recovery through the Stern-Gerlach Effect

Richard Barney

A senior thesis submitted to the faculty of
Brigham Young University
in partial fulfillment of the requirements for the degree of
Bachelor of Science

Jean-François Van Huele, Advisor

Department of Physics and Astronomy
Brigham Young University

Copyright © 2018 Richard Barney

All Rights Reserved

ABSTRACT

Quantum Erasure and Coherence Recovery through the Stern-Gerlach Effect

Richard Barney

Department of Physics and Astronomy, BYU

Bachelor of Science

The phenomenon of quantum erasure has long been a curiosity in the field of quantum mechanics because it appears to allow future entangling measurements to affect a system's behavior in the past. A consequence of quantum erasure is the modification of the wave and particle behaviors of quantum objects. This thesis examines this effect in the context of an eraser which uses the Stern-Gerlach effect to create entanglement. We employ analytic and algebraic methods to determine how the wavefunction of a quantum object evolves over time in such a system. We quantify the wave and particle behaviors in the system through coherence and distinguishability respectively. We find that the erasure process initially destroys the coherence of the object, but each spin substate may recover a degree of coherence. The degree of coherence recovered depends on the Stern-Gerlach fields' inhomogeneity orientations and the magnitude of the quantum object's spin. Full coherence can always be recovered with proper inhomogeneity orientations for spin-1/2 objects. There is only one case which allows for spin-1 objects to recover full coherence. Objects with spin values greater than 1 cannot recover full coherence and the maximum recoverable coherence decreases for greater spin values. These are important considerations when it is necessary to create a quantum state with a certain degree of coherence.

Keywords: quantum coherence, Stern-Gerlach, quantum erasure, wave-particle duality

ACKNOWLEDGMENTS

Many thanks to Delaney Barney for her support and suggestions as I completed this work.

Contents

Table of Contents	iv
List of Figures	v
1 Introduction	1
1.1 Overview of Thesis	1
1.2 Motivation	2
1.3 Background Information	2
1.3.1 Heisenberg Uncertainty	2
1.3.2 Wave-Particle Duality	4
1.3.3 Quantum Erasure	6
1.3.4 The Stern-Gerlach Effect	9
1.4 Summary of Findings	11
2 Methods	13
2.1 Evolution of Gaussian Wavepackets	14
2.2 Evolution of Arbitrary Wavefunctions	15
2.3 Changes in Field Inhomogeneity Direction	17
2.4 Quantification of Wave Behavior	18
3 Results and Discussion	20
3.1 Time Evolution of Probability Density	20
3.2 Changes in Coherence	23
3.3 Conclusion	27
Appendix A Simulation Code	29
Bibliography	38
Index	41

List of Figures

1.1	Young's double slit experiment for particles and waves	5
1.2	A quantum erasure scheme using entangled photons	7
1.3	The Stern-Gerlach effect for spin-1/2 quantum objects	10
1.4	A modified Stern-Gerlach apparatus for quantum erasure	11
3.1	Time evolution of the probability distribution for a spin-1/2 quantum object with orthogonal subsequent magnetic field orientations	21
3.2	Time evolution of the probability distribution for a spin-1/2 quantum object with non-orthogonal subsequent magnetic field orientations	24
3.3	Time evolution of the probability distribution for a spin-1 quantum object with orthogonal subsequent magnetic field orientations.	25
3.4	Recovered coherence for spin-1/2 quantum objects	26
3.5	Recovered coherence for spin-1 quantum objects	26
3.6	Recovered coherence for spin-3/2 quantum objects	27

Chapter 1

Introduction

1.1 Overview of Thesis

This thesis examines the connection between wave-particle duality and quantum erasure in the context of a Stern-Gerlach quantum erasure setup. The first chapter of this thesis describes the purpose and motivation for this study and covers relevant background information such as the Heisenberg uncertainty principle, wave-particle duality, quantum erasure, quantum coherence, and the Stern-Gerlach effect. It also briefly summarizes the main results of the study. Chapter 2 discusses the mathematical methods used to determine the time-evolution of quantum objects as they pass through a Stern-Gerlach quantum eraser. It also discusses how quantum coherence is defined and calculated. Chapter 3 discusses how the methods of Chapter 2 were applied in this study and analyzes the results. The code used to carry out time-evolution simulations and plot the resulting probability distributions is included in Appendix A.

1.2 Motivation

Quantum erasure is one of the most surprising phenomena in quantum information theory. It arises from the fact that making a measurement on a quantum system can actually erase information that was previously available in the system. This can cause some subsets of quantum objects in the system to behave as if no information was initially available. This phenomenon is sometimes interpreted as evidence that future events may affect the past. While quantum erasure does not actually violate causality,¹ it is a unique resource that has been used in only a limited number of applications. It can be used in some cases to increase microscopic resolution by an order of magnitude.² Recent research has examined the possibility of using quantum erasure to increase the security of quantum communication schemes such as quantum key distribution.³ This thesis examines a specific implementation of a quantum eraser which uses the Stern-Gerlach effect to create and then destroy information about the position of quantum objects. While such a setup is not convenient for quantum communication or computation schemes, it is ideal for exploring the connection between quantum erasure and the wave-particle duality principle.

1.3 Background Information

1.3.1 Heisenberg Uncertainty

One of the most fundamental principles in quantum theory is Heisenberg uncertainty, which places a limit on how much information can be simultaneously known about incompatible observables of a system. The classic example is the duality relationship between knowledge of a quantum object's position and knowledge of its momentum. The more precisely the quantum object's position is known, the less precisely its momentum can be known and vice versa. This is expressed as the inequality $\Delta x \Delta p_x \geq \frac{\hbar}{2}$, where Δx and Δp_x are the uncertainties in the object's position and

momentum respectively. More generally, the uncertainties of any two observables a and b follow the relation $\Delta a \Delta b \geq \left| \frac{\langle [a,b] \rangle}{2i} \right|$. This quantum principle contrasts sharply with the implicit assumption of classical theories that all properties of a system can, in principle, be known simultaneously to arbitrary precision.

Initially Heisenberg uncertainty was thought to arise from the perturbing effect of measuring a quantum system. Consider a large classical object sitting in a dark room. If we want to measure the position of the object we could simply shine a light on the object and clearly determine its location. The act of shining the light on the object will not change its position. In fact, if no other forces act on the object, we can expect with high confidence that we will find the object in the same position every time we look. This is not the case with quantum objects. Suppose we want to measure the position of a single atom. To do so we decide to scatter a single photon off of the atom. By doing so we have measured the atom's position, but that measurement has necessarily affected the system. While scattering light off a macroscopic object will not appreciably alter its momentum, the momentum of a single atom can be changed significantly by a single scattered photon. In fact, Heisenberg used this general principle of measurement disturbance when deriving his uncertainty principle.

However, the uncertainty principle proves to be subtler than it first appears when indirect measurements are made through entanglement, which is simply a correlation between the observables of a system. Suppose we prepare our system in such a way that the momentum of a quantum object is entangled with another observable, say the momentum of a second object, through the principle of momentum conservation. By measuring the momentum of the second object, we gain information about the momentum of the first object without directly measuring it. However, despite the fact that there was no disturbing measurement on the first object, we still find that the information we have about the object's momentum puts a limit on how much we can know about the object's position. It is apparent from this scenario that the uncertainty principle cannot arise simply from direct

measurement disturbance.⁴ The principle describes a fundamental limit on how much information can be simultaneously available in a system, regardless of how that information might be collected. Since quantum waves often lose coherence when information is gathered through measurement, it seems that Heisenberg uncertainty and the wave/particle nature of quantum objects may be linked.⁵

1.3.2 Wave-Particle Duality

In classical physics there are two distinct kinds of objects: particles and waves. Particles (e.g. protons, electrons, atoms, etc.) have the property that they are localized at a particular position in space and have a definite trajectory. Waves (e.g. light, sound, etc.) are not localized in a particular position and can interfere with themselves. One of the most remarkable discoveries of quantum physics is that quantum objects exhibit both wave and particle properties.

A conceptually simple way to demonstrate the wave-like properties of a quantum object is to send it through a double slit as Thomas Young did with light. If the object is a particle, we expect most of the detections on the screen to be bunched around the two regions behind the slits as shown in Figure 1.1(a). However, we can take material objects, which are usually thought of as particles, and find values for the energy of the object, the width of the slits, and the slit separation distance, to obtain a pattern on the detection screen that is consistent with a self-interfering wave. Such a pattern is shown in Figure 1.1(b).

Similarly, massless quantum objects like light can be shown to have particle-like properties. An illustrative example is the photoelectric effect. The photoelectric effect causes electrons to be ejected from a material when light shines on it. Thinking about light as a wave, we might conclude that energy from the wave is exciting the electrons in the material, imparting to them enough energy to escape. This leads us to believe that the kinetic energy of the escaping electrons depends on the intensity of the light. However, if we keep the intensity of the light constant but vary the light's wavelength, we will find that there is a threshold frequency below which no electrons are ejected

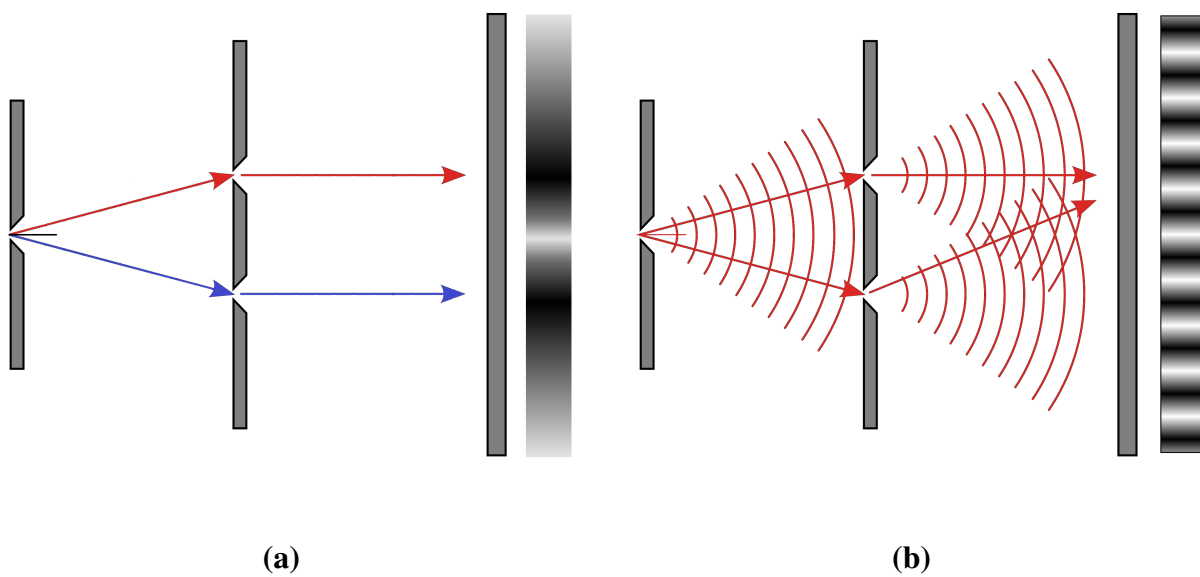


Figure 1.1 Young's double slit experiment for particles (a) and waves (b). In (a) each quantum object passes through only one slit (i.e. the blue path or the red path) and does not interfere with itself. Detections on the screen are bunched near the areas directly behind the slits. In (b) each quantum object passes through both slits simultaneously and interferes with itself. This causes a fringe pattern to appear on the detection screen.

from the material. This is because the light is not acting as a wave in this case, but as discrete particles called photons. The energy of each photon is given by the Planck relation $E = h\nu$ where ν is the frequency of the photon and h is Planck's constant. No matter how intense the light becomes, if the photons' frequency is below a certain threshold, no photon will have enough energy to eject an electron. The photoelectric effect, along with many other experimental results, strongly indicates that light can exhibit particle properties.

Curiously, quantum objects do not have to exhibit particle or wave behavior exclusively. They can actually display degrees of particle behavior and wave behavior simultaneously, with the constraint that the more particle-like the object becomes the less wave-like it becomes and vice versa. This principle, first clearly described by Bohr,⁶ is known as wave-particle duality.

Different approaches have been used to quantify the wave and particle behaviors of quantum objects. A common approach was developed by Englert.⁷ In this approach particle behavior is characterized by the amount of information available about the path of the object, quantified as path distinguishability D . Wave behavior is characterized by the fringe visibility V . Both of these measures can take any value between 0 and 1, with 1 corresponding to the greatest degree of a behavior. These values follow the duality relationship $D^2 + V^2 \leq 1$, which limits the degrees of wave and particle behaviors which can manifest simultaneously. Englert's approach applies only to two-path interferometers. In this thesis we will use the more general approach developed by Bera et al.⁸ This approach characterizes particle behavior by a similar measure of path distinguishability D_Q but characterizes wave behavior by quantum coherence C . This leads to the duality relationship $C + D_Q \leq 1$.

1.3.3 Quantum Erasure

The concept of quantum erasure was first clearly stated by Scully and Drühl⁴ in 1982. A simple example is reviewed here to demonstrate the principle. Consider the setup shown in Figure 1.2.

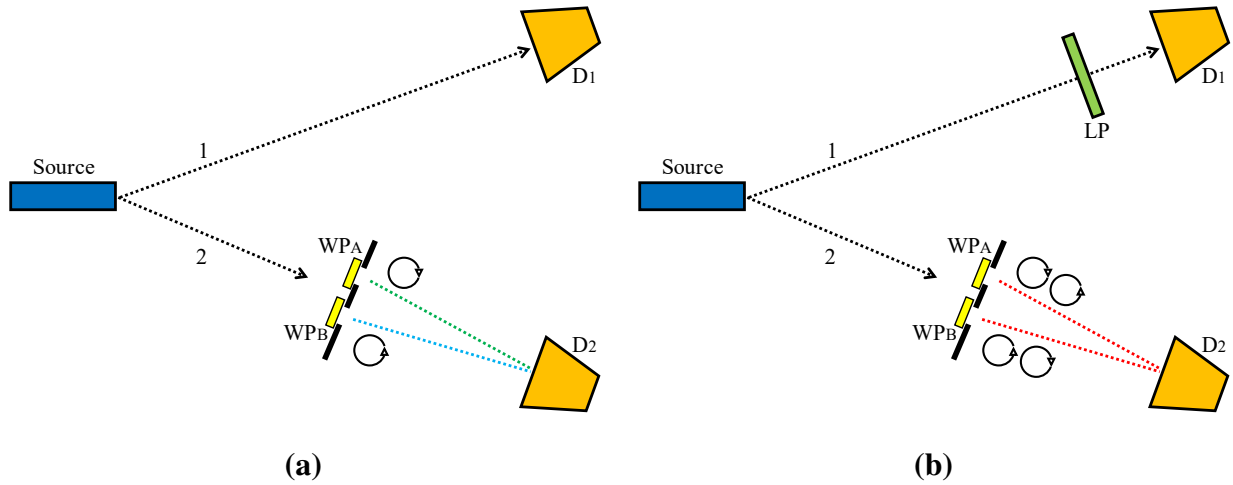


Figure 1.2 A simple quantum erasure scheme using entangled photons. Detectors D_1 and D_2 count coincident photon detections. In setup (a), waveplates WP_A and WP_B entangles the path photon 2 takes through the double slit with orthogonal circular polarizations. In the setup (b), the linear polarizer LP which photon 1 passes through causes the polarizations corresponding to the paths photon 2 takes to no longer be orthogonal.

A photon source emits two photons entangled in such a way that they have mutually orthogonal polarizations. If we take the polarization of the photon 1 to be in the horizontal direction, we can say that the initial state of the system is

$$|\Psi\rangle = |H\rangle_1 |V\rangle_2, \quad (1.1)$$

where $|H\rangle$ and $|V\rangle$ are the horizontal and vertical polarization states respectively. Photon 2 then encounters the double slit. There are waveplates on each of the slits so that only clockwise polarized light exits slit A and only counter-clockwise polarized light can exit slit B. This entangles the polarization of photon 2 with its path. The state of photon 2 becomes

$$|\Psi\rangle_2 = \frac{1}{\sqrt{2}}(|CW\rangle_2 |A\rangle + |CCW\rangle_2 |B\rangle), \quad (1.2)$$

where $|CW\rangle$ and $|CCW\rangle$ are the clockwise and counter-clockwise polarization states respectively. $|A\rangle$ and $|B\rangle$ denote the states of passing through slit A and slit B respectively. We can see from Eq. (1.2) that each path state is entangled with only one polarization state. This prevents self-interference

in photon 2.

We can change the setup slightly to have photon 1 pass through a linear polarizer some time after photon 2 encounters the double slit, making its state $|\Psi\rangle_1 = \frac{1}{\sqrt{2}}(|H\rangle + |V\rangle)$. Because the photons' polarizations are entangled, the polarization of photon 2 is changed too. The effect on the state of photon 2 is $|CW\rangle_2 \rightarrow \frac{1}{\sqrt{2}}(|CW\rangle_2 + |CCW\rangle_2)$ and $|CCW\rangle_2 \rightarrow \frac{1}{\sqrt{2}}(-|CW\rangle_2 + |CCW\rangle_2)$. This makes the state of photon 2 after it encounters the double slit

$$\begin{aligned} |\Psi\rangle_2 &= \frac{1}{\sqrt{2}} \left(\frac{1}{\sqrt{2}}(|CW\rangle_2 + |CCW\rangle_2)|A\rangle + \frac{1}{\sqrt{2}}(-|CW\rangle_2 + |CCW\rangle_2)|B\rangle \right) \\ &= \frac{1}{2} (|CW\rangle_2 (|A\rangle - |B\rangle) + |CCW\rangle_2 (|A\rangle + |B\rangle)). \end{aligned} \quad (1.3)$$

We can see that this entanglement causes interference terms to appear in the state of photon 2. Each polarization state is now entangled with both path states. Photon 2 now interferes with itself as if the polarizing masks were not there at all. This effect occurs despite the fact that the erasing event of photon 1 passing through the polarizer happened after photon 2 passed through the double slits and had to "decide" what it would do.⁴ A quantum eraser setup like this one was realized by Walborn et al.⁹ There are a variety of alternate implementations of a quantum eraser.^{1,4,10,11}

This example illustrates two important principles. First, it demonstrates that information is created and then destroyed in a quantum erasure scheme. When the photon 2 passes through the double slits, its polarization becomes entangled with its path. This means that if we measure the polarization of the photon before it reaches the detector screen, we would know which path it had taken. The photon has been tagged with path information. However, after the erasing event, measuring the polarization of the photon will not give us any path information. For either polarization, the photon has a 50% chance of coming from either slit. So the erasure event has, in a literal sense, erased the path information of the photon. Both the creation and the destruction of path information were done through entanglement.

The second important principle to note is that the erasure changed the wave and particle behavior of the second photon. In the setup without the linear polarizer for photon 1, photon 2 behaves as a

particle and does not interfere with itself. When the setup is altered so that photon 1 passes through the linear polarizer, photon 2 behaves as a wave exhibiting self-interference. The degree to which photon 2 behaves as a wave can be changed by changing the orientation of the linear polarizer. These principles will come into play as we examine quantum erasure with the Stern-Gerlach effect.

1.3.4 The Stern-Gerlach Effect

The original Stern-Gerlach experiment¹² was performed with silver atoms, which have the useful property of being electrically neutral but with nonzero angular momentum. This causes each atom to act as a magnetic dipole. As a beam of magnetic dipoles with random orientations passes through an inhomogeneous magnetic field, each dipole is deflected parallel to the inhomogeneity direction. Classical considerations lead us to believe that the amount of deflection for each dipole is proportional to the component of that dipole which is parallel to the inhomogeneity. This would lead to a continuous distribution of deflections when the beam is viewed as a whole.

Stern and Gerlach performed this experiment but found results inconsistent with the classical considerations. They observed that passing a beam of silver atoms through an inhomogeneous magnetic field caused the single beam to diverge into two beams and strike a detection screen at two distinct places, as seen in Figure 1.3. This is very different from the continuous distribution classical physics predicts. The reason for this discrepancy is the fact that the spectrum of angular momentum for quantum objects is discrete rather than continuous. This angular momentum turns out to be an intrinsic property of quantum objects and is known as spin. Silver atoms are spin-1/2 objects, which means their spin quantum number m_s can take the values $m_s = 1/2$ (spin up) or $m_s = -1/2$ (spin down). In general, the Stern-Gerlach effect will split a single beam into n beams, with

$$n = 2s + 1, \tag{1.4}$$

where s is the spin quantum number of the object.

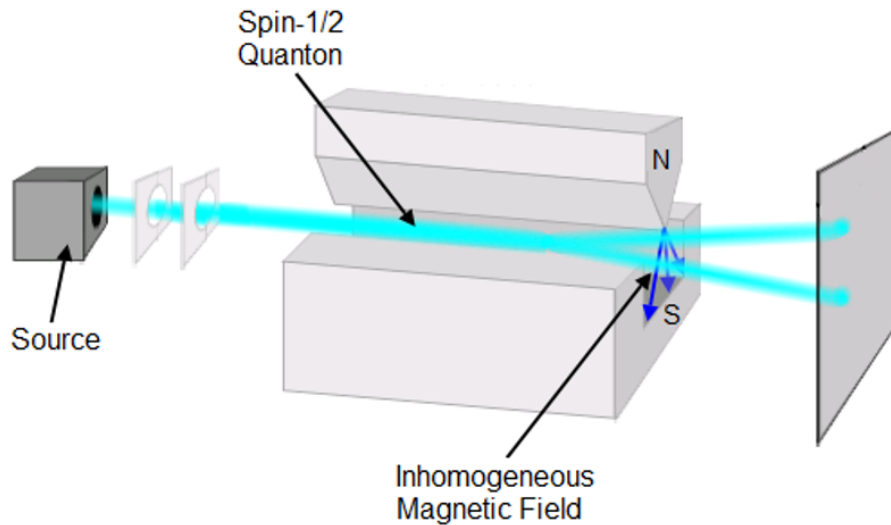


Figure 1.3 The Stern-Gerlach effect for spin-1/2 quantum objects. A beam of these objects passes through an inhomogeneous magnetic field, which splits the beam into two distinct beams.

Here the Stern-Gerlach effect has a similar role to that of the double slits with polarizers in Figure 1.2. The inhomogeneous magnetic field creates an entanglement between the spin of the quantum object and the path it takes. If a silver atom is observed taking the upper path, it must be spin up, and vice versa. This entanglement process suggests that the Stern-Gerlach effect can be used to create a quantum eraser.

Qureshi and Rahman¹³ proposed implementing such a quantum eraser by using two magnets to create two Stern-Gerlach fields with perpendicular inhomogeneity directions. The first magnet entangles the quantum object's spin with its position in the z -dimension. The second magnet is oriented perpendicularly to the first. It entangles the object's spin with its position in the x -dimension. However, the object's spin in x is not determined by its previous spin in z . For example, an object that takes the lower path and is spin down after passing through the first magnet has equal probabilities of being spin up or spin down in x after passing through the second magnet. Effectively, the second magnet is erasing the path information which was created by the first magnet. Due to this erasure,

the quantum object behaves as a wave, which creates an interference pattern on the detector screen.

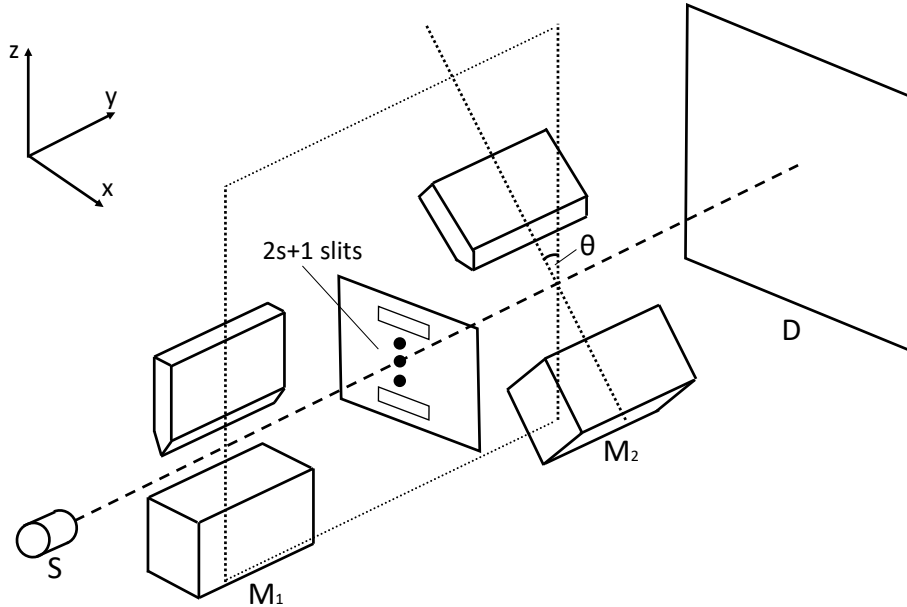


Figure 1.4 A variation on the Stern-Gerlach apparatus proposed by Qureshi and Rahman in Reference 12. Quantum objects are emitted from the source S . The first magnet M_1 entangles the object's spin with its position in z . The second magnet M_2 entangles the object's spin with its position in another direction. This erases some of the path information created by the first magnet. A set of self-interference patterns are observed on the detector screen D .

1.4 Summary of Findings

This thesis explores variations on the quantum eraser proposed by Qureshi and Rahman¹³ (pictured in Figure 1.4) and determines how the quantum coherence changes as these variations are made. The quantum coherence is an effective measure of the wave behavior of the objects in the system and depends on the orientation of the inhomogeneity of the second Stern-Gerlach field and the spin of the object. As the second field's inhomogeneity direction is rotated, the quantum coherence oscillates.

The spin of the object also determines the maximum amount of coherence which can be

recovered by the second magnet. For appropriate field orientations, full coherence can always be recovered for spin-1/2 quantum objects. Full coherence can be recovered for spin-1 objects if $m_s = 0$. If the spin of the object is greater than 1, full coherence cannot be recovered. In general, the higher the spin of the object, the lower the recoverable coherence.

Chapter 2

Methods

The Hamiltonian for a quantum object in a magnetic field is

$$H \doteq \frac{p^2}{2m} - (\boldsymbol{\mu} \cdot \mathbf{B}), \quad (2.1)$$

where p is the object's momentum, m is its mass, $\boldsymbol{\mu}$ is its magnetic moment and \mathbf{B} is the magnetic field. The magnetic field in a Stern-Gerlach apparatus can be approximated to be linearly inhomogeneous. Assuming the inhomogeneity is in the x -dimension gives $\boldsymbol{\mu} \cdot \mathbf{B} = \beta x \sigma_x$ where β is some constant and σ_x is the Pauli spin operator in the x -dimension. This leads to the Stern-Gerlach Hamiltonian

$$H \doteq \frac{p^2}{2m} - \beta x \sigma_x. \quad (2.2)$$

The purpose of Sections 2.1 and 2.2 is to use this Hamiltonian to determine how the wavefunction of a quantum object evolves over time in a Stern-Gerlach system. We first examine the case where the initial wavefunction is Gaussian and the Hamiltonian is time-independent. We then treat the more general case of an arbitrary initial wavefunction and a time-dependent Hamiltonian.

2.1 Evolution of Gaussian Wavepackets

Assuming that the initial wavefunction $\Psi(x, 0)$ of the quantum object is Gaussian allows the use of a method given by Tannor¹⁴ to find the wavefunction at later times. This method is based on the fact that a Gaussian wavepacket remains Gaussian as it evolves if the potential is of quadratic or lower power spatially. It can be seen from Eq. (2.2) that the potential in the Stern-Gerlach system is of first order in x . We take an initial wavefunction of the form

$$\Psi(x, 0) = N \exp \left[-\alpha_0 (x - x_0)^2 + \frac{i}{\hbar} p_0 (x - x_0) + \frac{i}{\hbar} \gamma_0 \right], \quad (2.3)$$

where α_0 is the width of the wavepacket, x_0 is the location of the center, p_0 is the average momentum, γ_0 is a phase term, and N is a normalizing factor. We can then assume that the wavefunction at later times will have the form

$$\Psi(x, t) = N \exp \left[-\alpha_t (x - x_t)^2 + \frac{i}{\hbar} p_t (x - x_t) + \frac{i}{\hbar} \gamma_t \right], \quad (2.4)$$

where α_t, x_t, p_t , and γ_t are functions of t . Writing the Gaussian wavepacket in this form has the advantage of making it simple to identify the average momentum (p_t) and location of the center of the wavepacket (x_t). α_t describes the width of the wavepacket and γ_t is a phase term.

The next step is to solve for the α_t, x_t, p_t , and γ_t . Inserting $\Psi(x, t)$ of Eq. (2.4) into Schrödinger's equation with the Hamiltonian given by Eq. (2.2) and equating coefficients leads to the set of coupled differential equations

$$\begin{aligned} \dot{\alpha}_t &= -\frac{2i\hbar}{m} \alpha_t^2 \\ \dot{p}_t &= \beta \sigma_x \\ \dot{x}_t &= \frac{p_t}{m} \\ \dot{\gamma}_t &= \frac{p_t^2}{2m} - \frac{\hbar^2}{m} \alpha_t + \beta \sigma_x x_t \end{aligned} \quad (2.5)$$

with the solutions

$$\begin{aligned}
\alpha_t &= \frac{\alpha_0}{1 + 2i\hbar t \alpha_0/m} \\
p_t &= \beta \sigma_x t + p_0 \\
x_t &= \frac{1}{m} \left(\frac{1}{2} \beta \sigma_x t^2 + p_0 t \right) + x_0 \\
\gamma &= \frac{i\hbar}{2} \ln \left(1 + \frac{2i\hbar \alpha_0 t}{m} \right) + \frac{p_0^2}{2m} t + \frac{1}{3m} \beta^2 t^3 + \beta \sigma_x \left(\frac{p_0}{m} t^2 + x_0 t \right) + \gamma_0.
\end{aligned} \tag{2.6}$$

With these explicit expressions, Eq. (2.4) can be used to describe the wavefunction of the quantum object for any time.

2.2 Evolution of Arbitrary Wavefunctions

A more general approach is necessary for the case of an arbitrary initial wavefunction where the magnitude of the magnetic field's inhomogeneity varies with time. The Hamiltonian for this time-dependent potential is

$$H \doteq \frac{p^2}{2m} - \beta(t)x\sigma_x. \tag{2.7}$$

Since this Hamiltonian is time-dependent, an advanced algebraic method¹⁵ is applied to solve for the wavefunction. In order to find the wavefunction as a function of time $\Psi(x, t)$ the time-evolution operator of the system must first be found. This operator may then be used to construct a propagator which serves as a spatial Green's function.

A Lie algebra \mathcal{A} is constructed using the terms of the Hamiltonian as the smallest generating set. From Eq. (2.7) it is seen that the smallest generating set of \mathcal{A} is $\{p^2, x\sigma_x\}$, so the generators of \mathcal{A} are

$$\mathcal{A}_G = \{p^2, \sigma_x x, p\sigma_x, 1\}. \tag{2.8}$$

The ansatz that the time evolution operator for the system has the form

$$U(t) \doteq e^{\alpha_1(t)\sigma_x x} e^{\alpha_2(t)p^2} e^{\alpha_3(t)p\sigma_x} e^{\alpha_4(t)} \tag{2.9}$$

can be used to find that the system's propagator is

$$\begin{aligned}
K(x, x') &= \langle x | U | x' \rangle \\
&= \frac{1}{2\hbar i \sqrt{\pi \alpha_2}} \exp \left\{ \frac{1}{4\hbar^2 \alpha_2} [x^2 + x'^2 + 2ix' \alpha_3 \sigma_x \hbar + \hbar^2 (4\alpha_2 \alpha_4 - \alpha_3^2 \sigma_x^2) \right. \\
&\quad \left. - 2x(x' + \sigma_x \hbar (i\alpha_3 - 2\hbar \alpha_1 \alpha_2))] \right\}.
\end{aligned} \tag{2.10}$$

In order to find the functions $\alpha_1(t), \dots, \alpha_4(t)$, Eq. (2.9) is inserted in the Schrödinger equation. The resulting expression is then simplified using the Baker-Campbell-Hausdorff identity¹⁶

$$e^{\lambda A} B e^{-\lambda A} \doteq B + \frac{\lambda}{1!} [A, B] + \frac{\lambda^2}{2!} [A, [A, B]] + \dots, \tag{2.11}$$

where A and B are elements of the Lie algebra and λ is a scalar. The result is the set of coupled differential equations

$$\begin{aligned}
\dot{\alpha}_1 &= \frac{i}{\hbar} \beta(t) \\
\dot{\alpha}_2 &= -\frac{i}{\hbar} \frac{1}{2m} \\
\dot{\alpha}_3 &= -2i\hbar \alpha_1 \dot{\alpha}_2 \\
\dot{\alpha}_4 &= \hbar^2 \alpha_1^2 \dot{\alpha}_2 - i\hbar \alpha_1 \dot{\alpha}_3,
\end{aligned} \tag{2.12}$$

with the solutions

$$\begin{aligned}
\alpha_1(t) &= \frac{i}{\hbar} \int_0^t \beta(t') dt' \\
\alpha_2(t) &= -\frac{i}{\hbar} \frac{t}{2m} \\
\alpha_3(t) &= \frac{i}{\hbar} \int_0^t t' \beta(t') dt' \\
\alpha_4(t) &= -\frac{i}{\hbar} \int_0^t t' \beta(t') \int_0^{t'} \beta(t'') dt'' dt'.
\end{aligned} \tag{2.13}$$

These solutions allow us to use the propagator in Eq. (2.10) as a spatial Green's function to find the time-evolved wavefunction, which is given by

$$\Psi(x, t) = \int_{-\infty}^{\infty} K(x, x') \Psi(x', 0) dx', \tag{2.14}$$

where $\Psi(x, 0)$ is the initial wavefunction.

Since this is the more general case, these results should match the results of the Section 2.1 when $\beta(t)$ is a constant function and $\Psi(x, 0)$ is Gaussian. In this case Eq. (2.10) becomes

$$K(x, x') = \sqrt{\frac{m}{2\pi i\hbar t}} \exp \left\{ -\frac{m(x-x')^2}{2i\hbar t} - \frac{\beta \sigma_x t (x+x')}{2i\hbar} + \frac{\beta^2 t^3}{24i\hbar m} \right\}, \quad (2.15)$$

which is the accepted propagator for a quantum object in a static Stern-Gerlach field.¹⁷ Using this propagator $K(x, x')$ and the initial Gaussian wavefunction $\Psi(x, 0)$ given by Eq. (2.3) in the integral of Eq. (2.14), we obtain the time-evolved Gaussian wavepacket $\Psi(x, t)$ given by Eq. (2.4) with the values of the parameters $(\alpha_t, x_t, p_t, \gamma_t)$ given by Eq. (2.6). So the results of this algebraic approach do indeed reduce to the results of Section 2.1 in the case of a static Stern-Gerlach field and a Gaussian initial wavefunction.

2.3 Changes in Field Inhomogeneity Direction

The results of the previous section can be used to find how the wavefunction of a quantum object evolves in a single magnetic field. However, interesting behavior can be found if we apply a series of Stern-Gerlach fields with their inhomogeneities in varying directions. In order to find how the quantum object evolves when a new field is applied, the wavefunction must be written in terms of the spin eigenstates parallel to the new field inhomogeneity.

We define θ as the difference between the directions of the inhomogeneities of the new field and the previous field. For the case of a spin-1/2 quantum object with $\theta = \pi/2$, it is not hard to see that $|S_x; +\rangle = \frac{1}{\sqrt{2}}(|S_z; +\rangle + |S_z; -\rangle)$ and $|S_x; -\rangle = \frac{1}{\sqrt{2}}(-|S_z; +\rangle + |S_z; -\rangle)$. For a quantum object with different spin, the basis transformation is not so intuitive. The general operator which effects the needed basis transformation is the rotation operator

$$R_\theta = \exp \left(-i\theta \frac{\hat{\mathbf{n}} \cdot \mathbf{S}}{\hbar} \right), \quad (2.16)$$

where \mathbf{S} is the spin operator and $\hat{\mathbf{n}}$ is the unit vector parallel to the axis about which the rotation is occurring. For our examination of the evolution of quantum objects in the xz -plane we have $\hat{\mathbf{n}} = \hat{\mathbf{e}}_y$.

The wavefunction expressed in a basis u which is rotated θ from the basis v is given by

$$\Psi_u = R_\theta \Psi_v. \quad (2.17)$$

We can find how the wavefunction evolves over changes in the inhomogeneity direction by using one of the methods presented in Sections 2.1 and 2.2 up to the time of the change, applying R_θ to the wavefunction, and using that state as a new initial wavefunction. In this way the evolving wavefunction can be found as any number of Stern-Gerlach fields are applied.

2.4 Quantification of Wave Behavior

It is the change in the direction of the inhomogeneity of the field which changes the degree of wave and particle properties of each quantum object in the system. This section discusses a method of quantifying the amount of each property.

The particle nature of the object is described by the distinguishability, which in this case is a measure of how much information is available about an object's spin given its position. Since the spin states are orthogonal, the distinguishability D_Q will be equal to the predictability P , which is the probability of randomly correctly guessing the spin of the quantum object in the magnetic field by observing its position while it was being acted on by the previous field. We define the distinguishability/predictability as

$$D = P = 1 - \frac{1}{n-1} \sum_{i \neq j} |c_i| |c_j| \quad (2.18)$$

as given by Qureshi et al.,¹⁸ where c_i is the amplitude of each possible spin eigenstate and $n = 2s + 1$ with s being the spin number of the quantum object. The number of "options" of spin eigenstates the object has is given by n .

The wave behavior can be described by the quantum coherence of the state. We adopt the definition of coherence given by Baumgratz et al.¹⁹ This definition quantifies coherence as the sum of the l_1 -norms of the off-diagonal elements of the state's density matrix ρ in the spin representation,

$$\begin{aligned} C &= \frac{1}{n-1} \sum_{i \neq j} |\rho_{ij}| \\ &= \frac{1}{n-1} \sum_{i \neq j} |\langle i | \rho | j \rangle|, \end{aligned} \quad (2.19)$$

where $\rho_{ij} = \langle i | \rho | j \rangle$ with $|i\rangle$ and $|j\rangle$ being spin eigenstates. Given that $|\langle i | \rho | j \rangle| = |c_i| |c_j|$, it is simple to show that the coherence and distinguishability follow the duality relation

$$C + D_Q = 1 \quad (2.20)$$

as expected of pure states.

The coherence C of a quantum object after it has been acted on by one or more magnetic fields is always 0, meaning that the quantum object as a whole is acting as a particle. This might seem to indicate that a Stern-Gerlach field does not actually erase the path information created by the previous field, preventing the recovery of coherence. However, the substates of the object associated with the different spin eigenstates can, in fact, have nonzero coherence. The m^{th} spin substate is given by

$$|\Psi_{\text{sub},m}\rangle = \frac{\langle S_m | \Psi \rangle}{|\langle S_m | \Psi \rangle|}, \quad (2.21)$$

where $|S_m\rangle$ are the spin eigenstates of the system. The coherence of the m^{th} spin substate is then

$$C_m = \sum_{i \neq j} \langle i | \Psi_{\text{sub},m} \rangle \langle \Psi_{\text{sub},m} | j \rangle.$$

These results are used to determine the coherence of each spin substate as the second magnetic field is acting on the object. This effectively measures how much path information the second field has erased.

Chapter 3

Results and Discussion

3.1 Time Evolution of Probability Density

The methods discussed in Chapter 2 are used to determine how the wavefunction of each quantum object in the system evolves over time. We use these methods to plot the spatial probability distribution $|\Psi(x, z, t)|^2$ at various times, creating animations of the time evolution of the probability distribution of each quanton. We do this for various scenarios, extending results from previous work²⁰ by varying the angle between the field inhomogeneity directions and the spin of the quantum object. Figures 3.1-3.3 show stills of these animations for Gaussian wavepackets. The Gaussian wavepackets are used for these plots because they allow the effects of quantum erasure to be visually recognized more easily. In each of these plots $\hbar = m = 1$. The initial widths of the wavepackets have been set as $\alpha_x = \alpha_z = 3$. Each initial wavepacket initially has its momentum centered at 0 and its position centered at the origin.

Figure 3.1 shows the time-evolution of a spin-1/2 quantum object whose initial state is a Gaussian wavepacket and the inhomogeneity direction of the second field is at an angle $\pi/2$ to the first. The first field causes the wavepacket to split into two wavepackets with no interference between

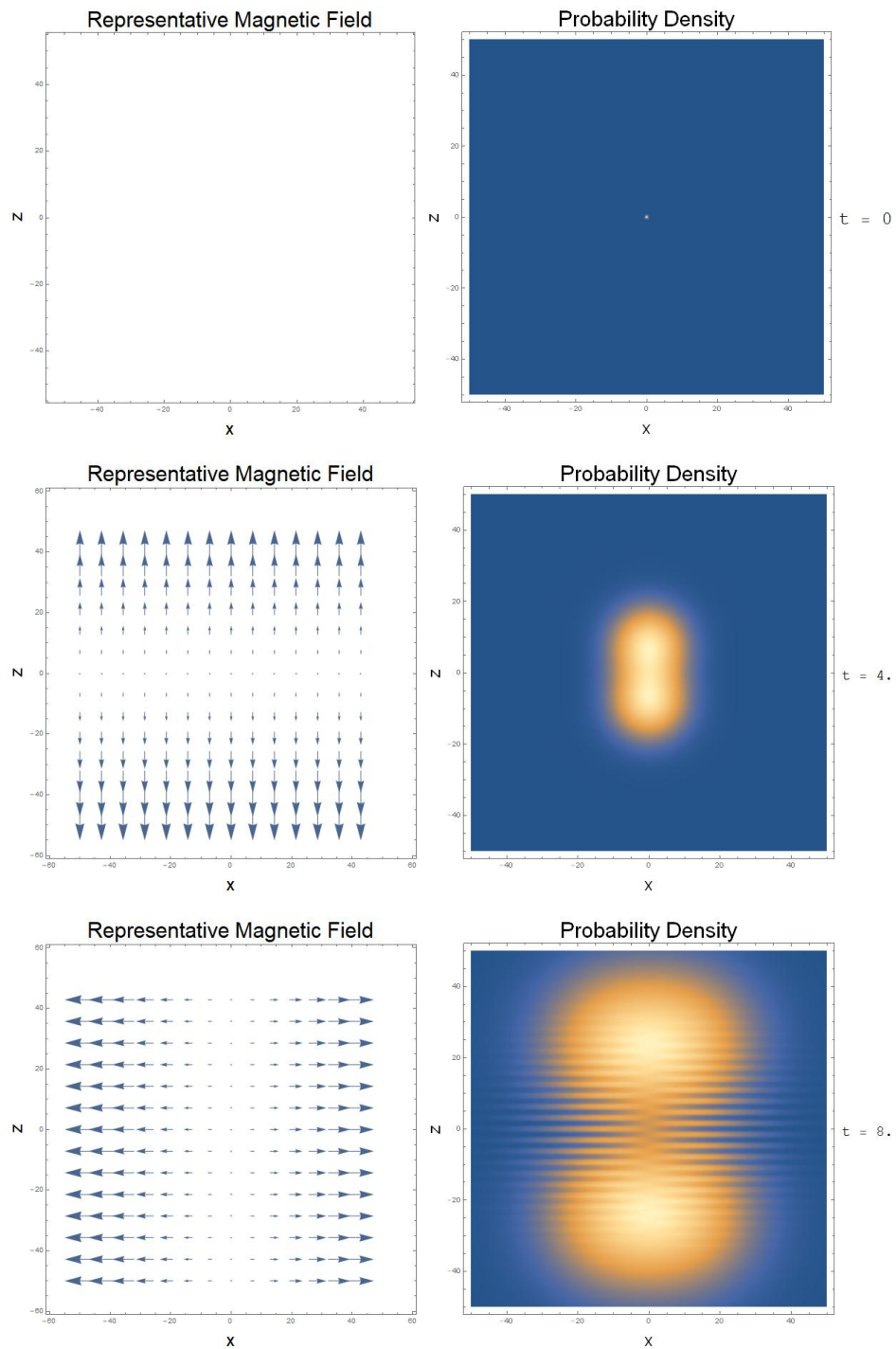


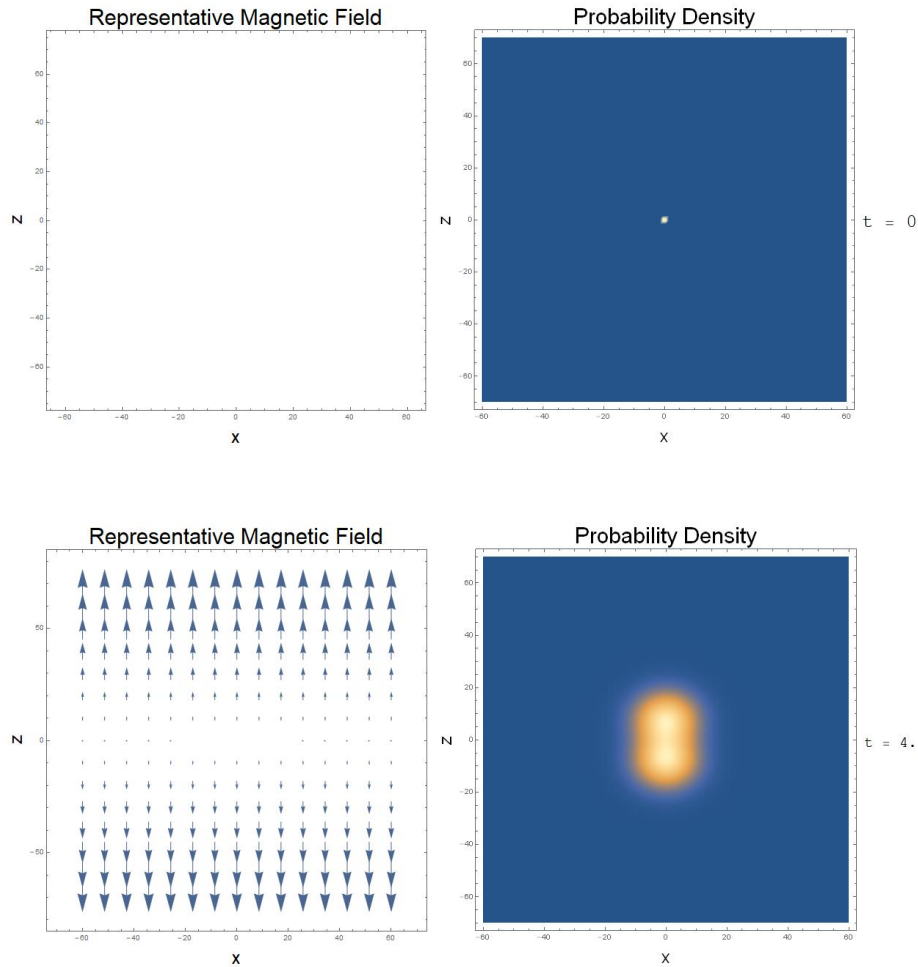
Figure 3.1 Time evolution of the probability distribution for a spin-1/2 quantum object with orthogonal subsequent magnetic field orientations. Horizontal fringes are formed.

them. The state of the object at this time is $|\Psi\rangle = \frac{1}{\sqrt{2}}(|\psi_{x+}\rangle|S_x, +\rangle + |\psi_{x-}\rangle|S_x, -\rangle)$. The object is behaving purely as a particle at this time. The second field causes the two wavepackets to split into a total of four. This time there is an obvious interference pattern between the wavepackets entangled with the same spin state. The state of the object is now $|\Psi\rangle = \frac{1}{2}(|\psi_{x+,z+}\rangle + |\psi_{x-,z+}\rangle)|S_z, +\rangle + \frac{1}{2}(|\psi_{x+,z-}\rangle + |\psi_{x-,z-}\rangle)|S_z, -\rangle$. The two "columns" of interference fringes are also seen to have a phase difference of π .

Figure 3.2 plots the same situation as Figure 3.1 except that the angle between the inhomogeneities of the second field and the first is now $\pi/4$. The probability distribution initially evolves as before where the first field splits the wavepacket in two and no interference occurs. But, when the second field is applied, the four resulting wavepackets move in different directions than they did in the previous case. For this reason, the interference pattern between wavepackets which have the same spin state is different than in Figure 3.1. However, the fringes in both cases are oriented in the same direction, despite the fact that the inhomogeneity of the second applied field is in different directions for the two cases. This is true in every case. The orientation of the fringe pattern is determined by the direction of the inhomogeneity of the previous field.

The spin of the quantum object can also be varied. A spin-1/2 system has two spin eigenstates, which cause the initial wavepacket to split in two when a Stern-Gerlach field is applied. A spin-1 system has three spin eigenstates, so we expect that the Stern-Gerlach field will split the initial wavepacket into three. Figure 3.3 shows that this is indeed the case. In this plot the angle between the inhomogeneities is $\pi/2$ as in Figure 3.1. When the second field is applied, three "columns" appear. However, only two of them have visible interference fringes. When the state of the object is examined we actually find that the two wavepackets in the center column do interfere with each other, but they are too far apart for this interference to be visible on the plot. This column only has two wavepackets instead of three like the others. The second field splits the three wavepackets into eight instead of nine as we might expect. This suggests that the coherence recovered through

applying the second field may not recover as much coherence as in the spin-1/2 case.²¹



3.2 Changes in Coherence

The amount of recovered coherence may be determined for all possible scenarios by using Eq. (2.19) to find the coherence as a function of the angle θ between inhomogeneity directions for all spin quantum numbers s and m_s . Each m_s corresponds to a "column" of fringes as seen in Figures 3.1-3.3. Figures 3.4-3.6 plot the recovered coherence as a function of θ for all the cases with $s = 1/2$, $s = 1$, or $s = 3/2$.

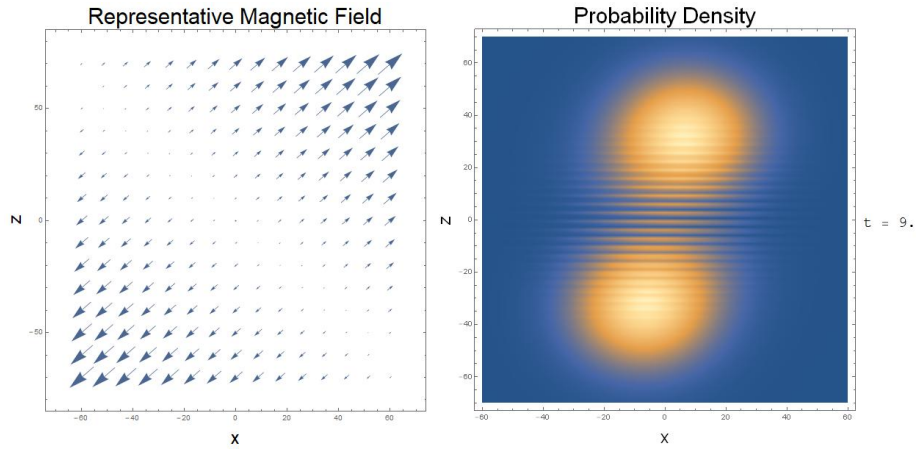


Figure 3.2 Time evolution of the probability distribution for a spin-1/2 quantum object with non-orthogonal subsequent magnetic field orientations. The wavepackets are moving diagonally in the second field but the fringes are oriented horizontally.

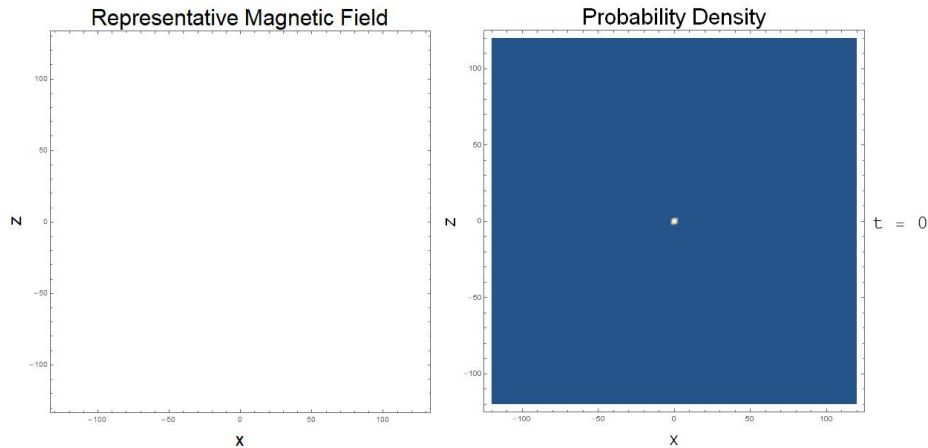


Figure 3.4 shows that each spin substate can recover full coherence when $\theta = \pi/2$ or $\theta = 3\pi/2$. In contrast, Figure 3.5 shows that full coherence can only be obtained by the $m_s = 0$ substate. This is achieved when $\theta = \arctan(\sqrt{2}), \pi - \arctan(\sqrt{2}), \pi + \arctan(\sqrt{2}),$ or $2\pi - \arctan(\sqrt{2})$. This substate has four maxima in contrast to the two maxima for the $s = 1/2$ case. Figure 3.6 shows that for $s = 3/2$, it is not possible to regain full coherence in this quantum eraser scheme. This is true in general for objects with $s > 1$. The $m_s = \pm 1/2$ cases have six maxima. The number of maxima increases with s . For each s , the spin substates with m_s values that are the least in magnitude have the largest number of maxima.

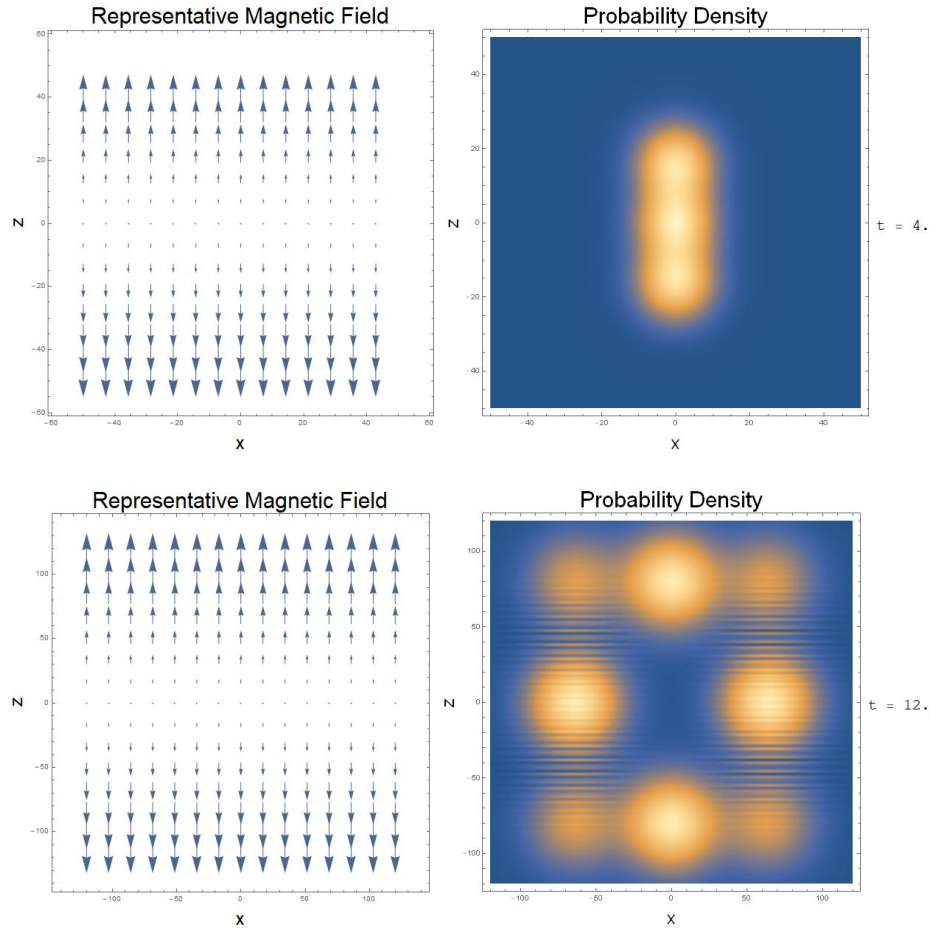


Figure 3.3 Time evolution of the probability distribution for a spin-1 quantum object with orthogonal subsequent magnetic field orientations. Eight wavepackets appear and fringes are formed.

The restrictions on the amount of coherence which can be recovered by the quantum eraser are connected to the dimensionality of the spin vector space. For spin-1/2 quantum objects the spin vector space is two dimensional. This means that any vector in the space can be transformed into a balanced superposition of orthogonal basis vectors by some rotation. This is why spin-1/2 quanta can always recover full coherence. The same is not true for quantum objects with higher spins and higher dimensional spin vector spaces. The rotation operator in Eq. (2.16) cannot transform all vectors into an equally balanced superposition in these cases. The $s = 1, m_s = 0$ case shown

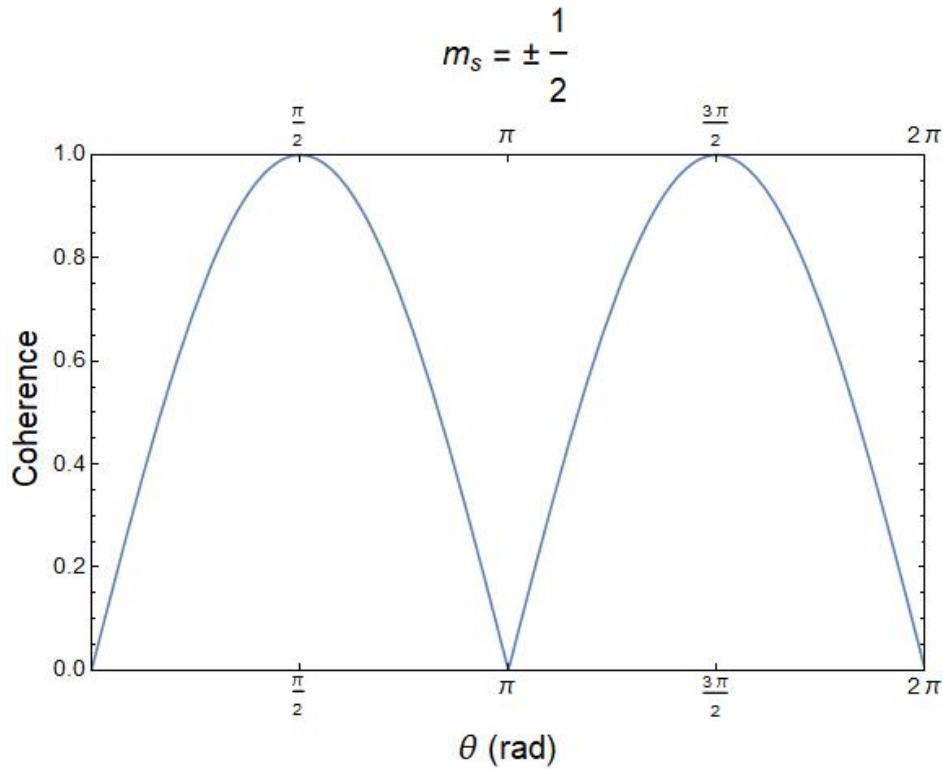


Figure 3.4 Recovered coherence for spin-1/2 quantum objects. Full coherence recovery occurs at $\theta = \pi/2$ and $\theta = 3\pi/2$.

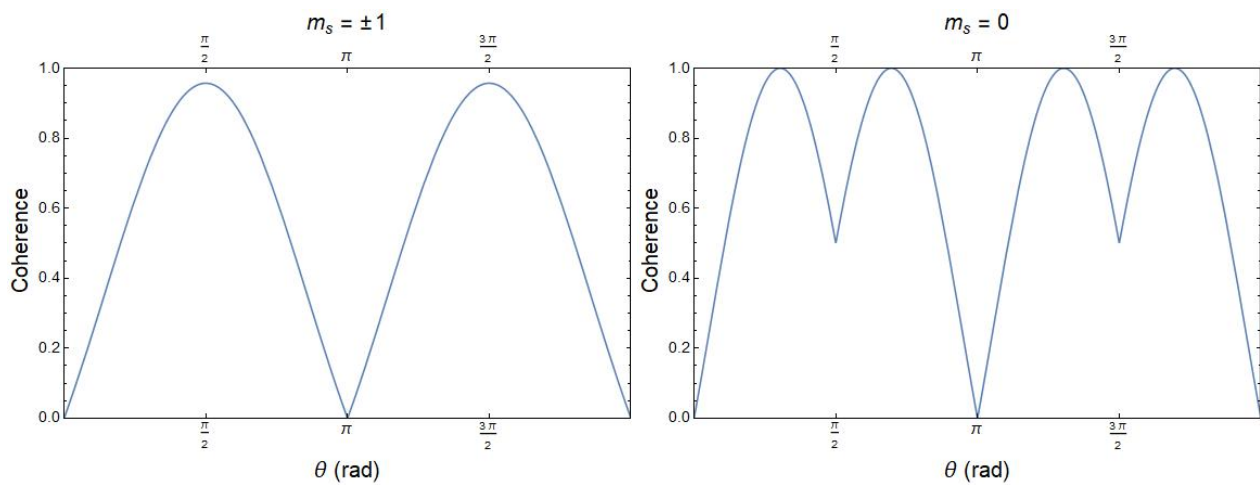


Figure 3.5 Recovered coherence for spin-1 quantum objects. For the substate $m_s = 0$, full coherence recovery occurs at $\theta = \arctan(\sqrt{2})$, $\pi - \arctan(\sqrt{2})$, $\pi + \arctan(\sqrt{2})$, and $2\pi - \arctan(\sqrt{2})$.

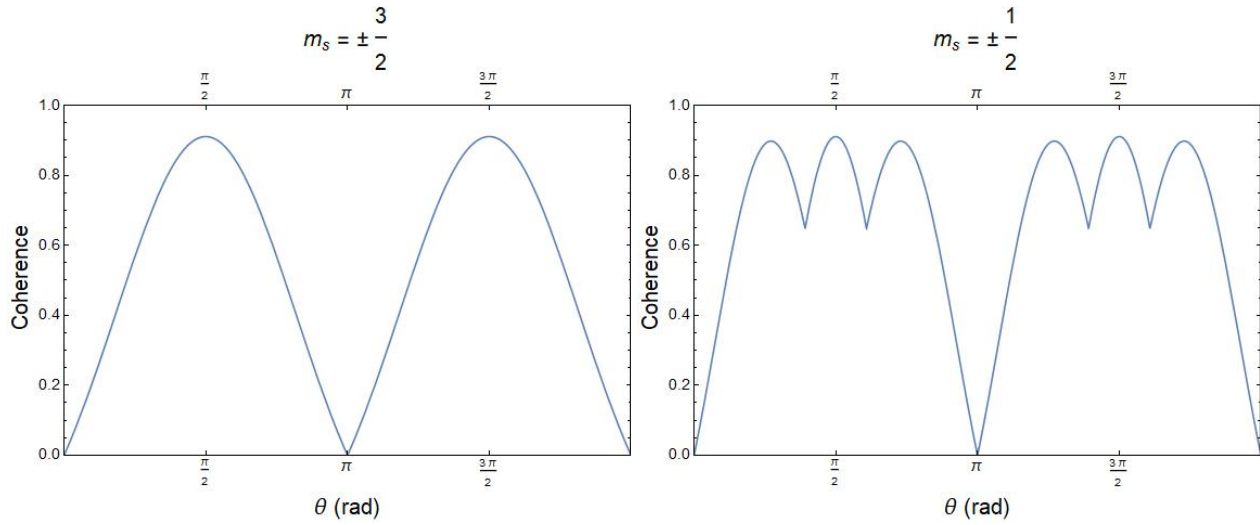


Figure 3.6 Recovered coherence for spin-3/2 quantum objects. Full coherence recovery is not possible.

in Fig. 3.5 shows that there still may be situations in which full coherence can be recovered for quantum object with higher spin numbers, but these situations are not guaranteed. If the quantum objects were emitted from the source in some state other than a balanced superposition of spin eigenstates, the angles and combinations of quantum numbers that lead to full coherence recovery would change.

3.3 Conclusion

In conclusion, we have found that the Stern-Gerlach effect can be used to implement a quantum erasure scheme. Applying one field to the quantum object entangles its position in the direction of the field inhomogeneity with the spin of the object. This causes the object to behave as a particle. Applying a second field entangles the object's spin with its position in a new direction. This second entanglement can either entirely or partially lift the previous entanglement, causing the object to regain wave behavior in the form of self-interference.

This wave behavior can be quantified using the L1-norm definition of quantum coherence in Eq.

(2.19). We found that the coherence recovered by applying the second field depends on the spin of the object and the angle between the inhomogeneity direction of the second field and the first. Full coherence can be regained for all spin substates when $s = 1/2$. This is not guaranteed for quantum objects with higher spin numbers due to the dimensionality of their spin vector spaces.

Appendix A

Simulation Code

This appendix lists the code I developed in a Mathematica notebook to simulate the evolution of Gaussian wavepackets. It uses the method outlined in Section 2.1. The values under the "Inputs" section should be set by the user and then the entire notebook should be evaluated. The result will be an exported .gif file depicting the evolution of the quantum object.

```
atime = AbsoluteTime[];  
Needs["CompiledFunctionTools"]
```

Inputs

```
doExport = False;  
name = "name.gif";
```

Slope of Magnitude and Direction

$$\beta_s[t_]=\{2,2,2,2\}$$

$$\theta_s=\{\text{Pi}/2,0,\text{Pi}/2,0\}$$

$$ts=\{0,4,8,12\}$$

$$\{\text{Length}[\beta_s[t]],\text{Length}[\theta_s],\text{Length}[ts]\}$$

x dimension parameters

$$N_x = 1;$$

$$\alpha_{x0} = 3;$$

$$p_{x0} = 0;$$

$$x_0 = 0;$$

$$\gamma_{x0} = 0;$$

z dimension parameters

$$N_z = 1;$$

$$\alpha_{z0} = 3;$$

$$p_{z0} = 0;$$

$$z_0 = 0;$$

$$\gamma_{z0} = 0;$$

Other Parameters

$$\text{spin} = 1;$$

$$\hbar = 1;$$

$$m = 1;$$

PlotBoundaries

$x_{\min} = -50;$

$x_{\max} = 50;$

$z_{\min} = -50;$

$z_{\max} = 50;$

$t_{\max} = 16;$

$\tau = 4;$

Convert To Float

$\{\beta_s[t], \theta_s, ts, \text{ent}, N_x, \alpha_{x0}, p_{x0}, x_0, \gamma_{x0}, N_z, \alpha_{z0}, p_{z0}, z_0, \gamma_{z0}, \hbar, m, x_{\min}, x_{\max},$
 $z_{\min}, z_{\max}, t_{\max}, \tau\} =$

$N[\{\beta_s[t], \theta_s, ts, \text{ent}, N_x, \alpha_{x0}, p_{x0}, x_0, \gamma_{x0}, N_z, \alpha_{z0}, p_{z0}, z_0, \gamma_{z0}, \hbar, m, x_{\min},$
 $x_{\max}, z_{\min}, z_{\max}, t_{\max}, \tau\}]$

Calculations

AppendTo[ts, Infinity];

$j = \text{spin};$

$\psi_s = \{\};$

$\psi_{2s} = \{\};$

$\psi_0[x_, z_] = \text{Exp}[-\alpha_{x0}(x - x_0)^2 + I/\hbar p_{x0}(x - x_0) + I/\hbar \gamma_{x0}] *$

$\text{Exp}[-\alpha_{z0}(z - z_0)^2 + I/\hbar p_{z0}(z - z_0) + I/\hbar \gamma_{z0}]$

$\text{prob}_0[x_, z_] = \text{Abs}[\psi_0[x, z]]^2$

$\text{basisshift} = \text{Compile}[\{\{j, _Real\}, \{\theta, _Real\}\}, \text{Module}[\{\},$

$n = 2j + 1;$

```

Jp = Table[0, {m, 1, n}, {k, 1, n}];
Jm = Jp;
For [m = 1, m < n, m++, (*Create J_- and J_+ matrices*)
Jp[[m, m + 1]] = Sqrt[j(j + 1) - (j - m)(j - m + 1)];
Jm[[m + 1, m]] = Sqrt[j(j + 1) - (j - (m - 1))(j - m)];
];
Jy = -I/2(Jp - Jm); (*Create J_y matrix*)
U = Sum[1/n!(-Iθ)^n MatrixPower[Jy, n], {n, 1, Infinity}] + IdentityMatrix[Round[n]]//
FullSimplify; (* Create rotation matrix *)
Chop[Re[U]]
], {{U, _Complex, 2}}
]
Monitor[For[i = 1, i < Length[ts], i++, (* execute for every transition time listed *)
βx[t_] = βs[t][[i]] Cos[θs[[i]]];
(* Create list of inhomogeneity strengths in x direction *)
βz[t_] = βs[t][[i]] Sin[θs[[i]]];
(* Create list of inhomogeneity strengths in z direction *)
σθ = Reverse[Table[n, {n, -j, j}]]; (* Create list of σ eigenvalues *)
αxt =  $\frac{\alpha x_0}{2I\hbar\alpha x_0/m+1}$ ; (* Find evolved αxt value *)
αzt =  $\frac{\alpha z_0}{2I\hbar\alpha z_0/m+1}$ ; (* Find evolved αzt value *)
If[Length[Flatten[{x0}]] ≤ 1, (* Check if this is the first evolution *)
xt =  $\frac{1}{m}(1/2\beta x[t]\sigma\theta t^2 + px_0 t) + x_0$ ; (* evolve xt *)
zt =  $\frac{1}{m}(1/2\beta z[t]\sigma\theta t^2 + pz_0 t) + z_0$ ; (* evolve zt *)
pxt = βx[t]σθ t + px0; (* evolve pxt *)
pzt = βz[t]σθ t + pz0; (* evolve pzt *)

```

$$\gamma_{xt} = \frac{\hbar}{2} \text{Log} \left[1 + \frac{2\hbar\alpha x_0 t}{m} \right] + \frac{1}{3m} \beta_x[t]^2 \sigma \theta^2 t^3 + \frac{1}{m} \beta_x[t] \sigma \theta p_{x0} t^2 + \frac{p_{x0}^2}{2m} t +$$

$\beta_x[t] \sigma \theta x_0 t + \gamma_{x0}; (* \text{ evolve } \gamma_{xt} *)$

$$\gamma_{zt} = \frac{\hbar}{2} \text{Log} \left[1 + \frac{2\hbar\alpha z_0 t}{m} \right] + \frac{1}{3m} \beta_z[t]^2 \sigma \theta^2 t^3 + \frac{1}{m} \beta_z[t] \sigma \theta p_{z0} t^2 + \frac{p_{z0}^2}{2m} t +$$

$\beta_z[t] \sigma \theta z_0 t + \gamma_{z0}; (* \text{ evolve } \gamma_{zt} *)$

,

(* If this is not the first evolution execute this *)

$\text{fx0} = \text{Flatten}[x0]; (* \text{ flatten list of initial conditions} *)$

$\text{fz0} = \text{Flatten}[z0];$

$\text{fpx0} = \text{Flatten}[p_{x0}];$

$\text{fpz0} = \text{Flatten}[p_{z0}];$

$\text{f}\gamma_{x0} = \text{Flatten}[\gamma_{x0}];$

$\text{f}\gamma_{z0} = \text{Flatten}[\gamma_{z0}];$

$\{\text{xt}, \text{zt}, \text{p}_{xt}, \text{p}_{zt}, \gamma_{xt}, \gamma_{zt}\} = \{\{\}, \{\}, \{\}, \{\}, \{\}, \{\}\};$

(* initialize evolved values as empty sets *)

$\text{For}[q = 1, q \leq \text{Length}[\text{fx0}], q++, (* \text{ iterate over each element in initial conditions} *)$

$\text{AppendTo}[\text{xt}, \frac{1}{m}(1/2\beta_x[t] \sigma \theta t^2 + \text{fpx0}[[q]]t) + \text{fx0}[[q]]; (* \text{ Evolve xt} *)$

$\text{AppendTo}[\text{zt}, \frac{1}{m}(1/2\beta_z[t] \sigma \theta t^2 + \text{fpz0}[[q]]t) + \text{fz0}[[q]]; (* \text{ evolve zt} *)$

$\text{AppendTo}[\text{p}_{xt}, \beta_x[t] \sigma \theta t + \text{fpx0}[[q]]; (* \text{ evolve p}_{xt} *)$

$\text{AppendTo}[\text{p}_{zt}, \beta_z[t] \sigma \theta t + \text{fpz0}[[q]]; (* \text{ evolve p}_{zt} *)$

$\text{AppendTo}[\gamma_{xt}, \frac{\hbar}{2} \text{Log} \left[1 + \frac{2\hbar\alpha x_0 t}{m} \right] + \frac{1}{3m} \beta_x[t]^2 \sigma \theta^2 t^3 + \frac{1}{m} \beta_x[t] \sigma \theta \text{fpx0}[[q]]t^2 +$
 $\frac{\text{fpx0}[[q]]^2}{2m} t + \beta_x[t] \sigma \theta \text{fx0}[[q]]t + \text{f}\gamma_{x0}[[q]]; (* \text{ evolve } \gamma_{xt} *)$

$\text{AppendTo}[\gamma_{zt}, \frac{\hbar}{2} \text{Log} \left[1 + \frac{2\hbar\alpha z_0 t}{m} \right] + \frac{1}{3m} \beta_z[t]^2 \sigma \theta^2 t^3 + \frac{1}{m} \beta_z[t] \sigma \theta \text{fpz0}[[q]]t^2 +$
 $\frac{\text{fpz0}[[q]]^2}{2m} t + \beta_z[t] \sigma \theta \text{fz0}[[q]]t + \text{f}\gamma_{z0}[[q]]; (* \text{ evolve } \gamma_{zt} *)$

];

];

```

normalization = 1/Sqrt[2j + 1];(* overall normalization determined by spin value *)
ψadd = Exp[-αxt(x - xt)^2 + I/ħpxt(x - xt) + I/ħγxt]*
Exp[-αzt(z - zt)^2 + I/ħpzt(z - zt) + I/ħγzt];
(* put together new state for this time period *)
While[N[Length[ψadd]] > 2j + 1,
(* do while the length of ψadd is greater than the number of spin eigenstates *)
ψadd = Partition[ψadd, 2j + 1];
(* partition ψadd into lists of length equal to the number of spin eigenstates *)
];
ψcopy = ψadd;(* make a copy of ψadd *)
For[p = 2., p <= Log[2j + 1, N[Length[Flatten[ψcopy]]]], p++,
(*Executewhile(2j + 1)^p ≤ Length[Flatten[ψadd]]*)
ψadd = basisshift[j, θs[[p - 1]] - θs[[p]].ψadd;(*applythe(p - 1)thbasisshift*)
ψadd = Diagonal[ψadd];(* Transpose ψadd and take the diagonal elements *)
];
ψadd = normalization * ψadd;(* final form of ψadd *)
next = {ψadd/.t → (t - ts[[i]]), ts[[i]] ≤ t < ts[[i + 1]]};
(* pair ψ add with the proper time domain *)
AppendTo[ψs, next];(* put ψadd in the list ψs *)
nextabs = {Total[Abs[ψadd]^2]/.t → (t - ts[[i]]), ts[[i]] ≤ t < ts[[i + 1]]};
(* use ψadd to find the probability distribution *)
AppendTo[ψ2s, nextabs];(* add nextabs to list ψ2s *)
If[ts[[i + 1]] ≠ Infinity, (*setinitialconditionstoevolvedparametersfor
nextloop*)
{αx0, αz0, x0, z0, px0, pz0, γx0, γz0} =

```

```

{ $\alpha_{xt}$ ,  $\alpha_{zt}$ ,  $x_t$ ,  $z_t$ ,  $p_{xt}$ ,  $p_{zt}$ ,  $\gamma_{xt}$ ,  $\gamma_{zt}$ }/ $t \rightarrow (ts[[i + 1]] - ts[[i]]);$ 
];
remrep = Length[ts] - 1 - i; (* keep track of how many loops are left *)
], remrep]
AbsoluteTime[] - atime
 $\psi[x_, z_, t_] = \text{Piecewise}[\psi_s];$ 
prob[x_, z_, t_] = Piecewise[ $\psi_{2s}$ ];

```

Plotting

```

plot0 =
Grid[
{{DensityPlot[Chop[prob0[x, z]], {x, xmin, xmax}, {z, zmin, zmax}, PlotRange → All,
PlotPoints → 130, PlotLabel → Style["Probability Density", 30, Black],
FrameLabel → {Style[x, 25, Black], Style[z, 25, Black]}, ImageSize → Large,
AxesLabel → Automatic], Style["t = 0", 25, Black]}}}
plots =
Monitor[
Table[
Grid[
{{DensityPlot[prob[x, z, t], {x, xmin, xmax}, {z, zmin, zmax}, PlotRange → All,
PlotPoints → 130, ImageSize → Large,
FrameLabel → {Style[x, 25, Black], Style[z, 25, Black]},
PlotLabel → Style["Probability Density", 30, Black]},
Style["t = " <> ToString[N[t, 2]], 20, Black]}}}], {t,  $\tau$ , tmax,  $\tau$ },

```

```

Round[(tmax - t)/τ];
PrependTo[plots, plot0];
arrows = {};
arrows =
Table[VectorPlot[{βs[t][[i]]Cos[θs[[i]]](Cos[θs[[i]]]x + Sin[θs[[i]]]z),
βs[t][[i]]Sin[θs[[i]]](Cos[θs[[i]]]x + Sin[θs[[i]]]z)}, {x, xmin, xmax},
{z, zmin, zmax}, FrameLabel → {Style[x, 25, Black], Style[z, 25, Black]},
ImageSize → Large, PlotLabel → Style["Representative Magnetic Field", 30, Black]],
{i, 1, (Length[ts] - 1)}];
combplots = {};
For[k = 1, k <= Length[plots], k++,
For[r = 1, r < Length[ts], r++,
If[(k - 1)τ >= ts[[r]] && (k - 1)τ < ts[[r + 1]],
AppendTo[combplots, Grid[{{arrows[[r]], plots[[k]]}}]];
];
];
];

```

Export

```

SetDirectory[NotebookDirectory[]]
Export[name <> ".gif", combplots]

```

Results

```

Animate[combplots[[u]], {u, 1, Length[combplots], 1}]

```

AbsoluteTime[] – atime

Speak["Evaluation Finished"]

Bibliography

- [1] Y.-H. Kim, R. Yu, S. P. Kulik, Y. Shih, and M. O. Scully, “Delayed “Choice” Quantum Eraser,” *Phys. Rev. Lett.* **84**, 1–5 (2000).
- [2] Y. Aharonov and M. Zubairy, “Time and the Quantum: Erasing the Past and Impacting the Future,” *Science* **307**, 875–9 (2005).
- [3] H. Salih, “Quantum Erasure Cryptography,” *Frontiers in Physics* **4**, 16 (2016).
- [4] M. O. Scully and K. Drühl, “Quantum eraser: A proposed photon correlation experiment concerning observation and "delayed choice" in quantum mechanics,” *Phys. Rev. A* **25**, 2208–2213 (1982).
- [5] S. Dürr and G. Rempe, “Can wave-particle duality be based on the uncertainty relation?,” *American Journal of Physics* **68**, 1021–1024 (2000).
- [6] N. Bohr, “The Quantum Postulate and the Recent Development of Atomic Theory,” *Nature* **121**, 580 (1928).
- [7] B.-G. Englert, “Fringe Visibility and Which-Way Information: An Inequality,” *Phys. Rev. Lett.* **77**, 2154–2157 (1996).
- [8] M. N. Bera, T. Qureshi, M. A. Siddiqui, and A. K. Pati, “Duality of quantum coherence and path distinguishability,” *Phys. Rev. A* **92**, 012118 (2015).

- [9] S. P. Walborn, M. O. Terra Cunha, S. Pádua, and C. H. Monken, “Double-slit quantum eraser,” *Phys. Rev. A* **65**, 033818 (2002).
- [10] S. Dürr, T. Nonn, and G. Rempe, “Fringe Visibility and Which-Way Information in an Atom Interferometer,” *Phys. Rev. Lett.* **81**, 5705–5709 (1998).
- [11] A. G. Zajonc, L. J. Wang, X. Y. Zou, and L. Mandel, “Quantum Eraser,” *Nature* **353**, 507–508 (1991).
- [12] W. Gerlach and O. Stern, “Der experimentelle Nachweis der Richtungsquantelung im Magnetfeld,” *Zeitschrift für Physik* **9**, 349–352 (1922).
- [13] T. Qureshi and Z. Rahman, “Quantum Eraser Using a Modified Stern-Gerlach Setup,” *Prog. Theor. Phys.* **127**, 71–78 (2012).
- [14] D. Tannor, *Introduction to Quantum Mechanics* (University Science Books, 2007).
- [15] J. Wei and E. Norman, “Lie Algebraic Solution of Linear Differential Equations,” *Journal of Mathematical Physics* **4**, 575–581 (1963).
- [16] B. C. Hall, *Lie Groups, Lie Algebras, and Representations*, 2 ed. (Springer International Publishing, 2015).
- [17] B. C. Hsu, M. Berrondo, and J.-F. S. Van Huele, “Stern-Gerlach dynamics with quantum propagators,” *Phys. Rev. A* **83**, 012109 (2011).
- [18] T. Paul and T. Qureshi, “Measuring quantum coherence in multislit interference,” *Phys. Rev. A* **95**, 042110 (2017).
- [19] T. Baumgratz, M. Cramer, and M. B. Plenio, “Quantifying Coherence,” *Phys. Rev. Lett.* **113** (2014).

- [20] R. D. Barney and J.-F. S. Van Huele, “Probing Particle-wave Duality with the Stern-Gerlach Effect,” *Journal of the Utah Academy of Sciences, Arts & Letters* (2018).
- [21] R. D. Barney and J.-F. S. Van Huele, “Quantum Coherence Recovery through Stern-Gerlach Erasure,” submitted to *Physica Scripta* (2019).

Index

Baker-Campbell-Hausdorff Identity, 12

Coherence

 Definition, 15

 Recovery, 18

Distinguishability, 4, 14

Entanglement, 3, 6

Gaussian Wavepacket, 10

Green's Function, 11

Heisenberg Uncertainty, 2

Lie Algebra, 11

Particle-Wave Duality, 4

Photoelectric Effect, 4

Predictability, 14

Probability Distribution, 16

Propagator, 12

Quantum Erasure

 Through the Stern-Gerlach Effect, 8

 With Photons, 6

Rotation Operator, 13

Spin, 8

Stern-Gerlach Effect, 8

Stern-Gerlach Hamiltonian, 9

Substates, 15

Time Evolution Operator, 11

Visibility, 4

Wave-Particle Duality, 3

Young's Double-slit Experiment, 3